

We are IntechOpen, the world's leading publisher of Open Access books Built by scientists, for scientists

6,900

Open access books available

186,000

International authors and editors

200M

Downloads

Our authors are among the

154

Countries delivered to

TOP 1%

most cited scientists

12.2%

Contributors from top 500 universities



WEB OF SCIENCE™

Selection of our books indexed in the Book Citation Index
in Web of Science™ Core Collection (BKCI)

Interested in publishing with us?
Contact book.department@intechopen.com

Numbers displayed above are based on latest data collected.
For more information visit www.intechopen.com



Nonideal Solution Behavior in Forward Osmosis Processes Using Magnetic Nanoparticles

Jimmy D. Roach, Mandy M. Bondaruk and
Zain Burney

Additional information is available at the end of the chapter

<http://dx.doi.org/10.5772/intechopen.72474>

Abstract

Despite the tremendous progress made toward the realization of wider application for forward osmosis (FO) technologies, lack of suitable draw solutes that provide high water flux, low reverse solute flux, and facile recovery has hindered commercial development. An extensive variety of osmotic agents have been investigated during the past decade, and while simple inorganic salts remain the most widely used, organic-coated magnetic nanoparticles (MNPs) offer exploitable properties that hold great promise. In addition to size-mitigated reverse flux and low-cost recovery via magnetic separation, devitalized MNPs provide enhanced osmotic performance when compared to that of the ungrafted coating material at similar concentration levels, a consequence of greater nonideal solution behavior. This nonideality has been assessed using a simple, semiempirical model and is largely attributable to the increased solvent-accessible surface area and enhanced hydration. When attached to MNPs, polymers appear to behave osmotically as much smaller molecules, providing higher osmotic pressures and improved FO performance.

Keywords: forward osmosis, nonideality, draw solute, magnetic nanoparticles, counterion binding

1. Introduction

Forward osmosis (FO) exploits the natural osmotic pressure gradient between two fluids separated by a semi-permeable membrane to induce the net transport of solvent from a solution of lower osmotic pressure to that of higher osmotic pressure. The FO process appears to provide a low-energy, low-cost alternative to more conventional membrane-based separation methods and offers a myriad of potential applications in industries as diverse as desalination, oil and gas, and food processing [1, 2]. Despite advances made in FO during the past

decade, several challenges must still be overcome before more widespread relevance of the technology can be realized [3]. Recently, Shaffer et al. [4] provided a thermodynamic argument showing that FO-reverse osmosis (RO) desalination schemes cannot provide energy savings when compared to standalone RO. Although FO technology has been applied to a variety of water treatment strategies, draw solute inadequacies restrict its wider application [5, 6]. Mitigation of these inadequacies requires identification of draw solutions that achieve high osmotic pressure while minimizing reverse solute flux and also providing ease of recovery; the need for osmotic agents that allow for facile, inexpensive recovery remains paramount [7].

During the past decade, researchers have primarily focused their efforts in two areas, FO membrane production and draw solute identification. While considerable progress has been made toward the development of inexpensive and more robust membranes [8, 9], few commercially viable osmotic agents have been identified [10]. Desirable properties of the ideal osmotic agent are that it be nontoxic, inexpensive, stable, and highly water-soluble. In addition, the agent should have limited reverse draw solute flux, reduce internal concentration polarization (ICP), and be easily recoverable. Some osmotic agents and recovery schemes investigated to date include using inorganic salts with recovery by RO [11]; using poly(sodium acrylate) with recovery by ultrafiltration (UF) [12]; using thermoresponsive chitosan derivatives with recovery by aggregation at elevated temperature [13]; using ammonia-carbon dioxide with recovery by thermal separation [14]; using poly(N-isopropylacrylamide-co-acrylic acid) with recovery by heating and centrifugation [15]; using surfactants with recovery by UF [16]; and, using polyelectrolyte-based hydrogels with recovery by elevated temperature and pressure [17]. A critical review of what the authors term non-responsive and responsive draw solutes was recently provided by Cai and Hu [7].

Because they meet several of the aforementioned criteria, low reverse draw flux and easy recovery in particular, functionalized magnetic nanoparticles (MNPs) have garnered much attention as potential osmotic agents [18]. These MNPs typically incorporate a superparamagnetic core of Fe_3O_4 , with a magnetization value of 75.0 emu g^{-1} [19], onto which organic content is coated. Among the grafting agents that have been affixed to MNPs and investigated in FO processes are 2-pyrrolidine, triethylene glycol, and poly(acrylic acid) [20]; dextran [21]; poly(ethylene glycol) diacid [22]; poly(sodium acrylate) [23–25]; poly(sodium styrene-4-sulfonate) and poly(N-isopropylacrylamide) [26]; citrate [27]; hyperbranched polyglycerol [28]; and, citric acid and oxalic acid [19]. A primary advantage of using MNPs is their ease of recyclability through magnetic separation, although particle aggregation has been shown to diminish FO water flux values after multiple regeneration cycles [10]. Another benefit of derivatized MNPs is that they have been shown to provide higher osmotic pressures when compared to solutions of the organic grafting agents alone [20], an enhancement attributable to increased solution nonideality.

A solution behaves ideally when: (1) solute/solute, solvent/solvent, and solvent/solute interactions are identical and (2) all solute and solvent molecules occupy the same volume. Real solutions deviate from ideality due to an energetic nonequivalence in one or more of these interactions and/or volume occupancies are not identical. In aqueous solution, water molecules exhibit particularly strong hydrogen bonding with various organic functional groups, carboxylate moieties in particular [29]. Factors such as hydration, ion-pairing, and dimerization can

be significant contributors to thermodynamic nonideality [30] and can dramatically impact the osmotic performance of FO draw solutions.

A variety of models have been developed to explain the interesting osmotic behavior of concentrated solutions of proteins and other biological molecules [31–34]. The nonideal solution behavior of large biological molecules can lead to extreme changes in osmotic pressure. As an example, at a fixed protein concentration, the osmotic pressures of bovine serum albumin (BSA) solutions display greater than fivefold changes in the range $3 < \text{pH} < 8$ [32]. Such nonideality is generally attributable to variations in solvent-accessible surface area and polymeric segmental motion [35]. Models that adequately describe nonideal behavior in BSA and other polymer solutions provide a basis for explaining the unique osmotic properties of MNPs used in FO.

2. Osmotic theory

In order to function effectively as a draw agent in FO, the osmotic pressure of the draw solution must far exceed that of the feed solution. In terms of desalination, the draw must have an osmotic pressure significantly in excess of 7.7 atm in the case of a brackish feed, and in excess of 27 atm in the case of a seawater feed [4]. Because of their abilities to achieve high osmotic pressures while maintaining low solution viscosities, simple inorganic salts remain the most widely used draw agents. In addition, small ions tend to have greater diffusivity values thus moderating the effect of concentrative ICP. The strong affinity of small inorganic ions for water is revealed in their highly exothermic enthalpies of hydration [36]. This strong affiliation serves to significantly lower the chemical potential of water in draw solutions. Strong solvent/solute interactions provide high solution osmotic pressures while paradoxically making the regeneration of draw solute more difficult. Resolving this paradox has spurn interest in the development of easily removable draw agents that allow for regeneration through exploitation of solute size, thermal sensitivity, or magnetic properties. Of course, to be effective in FO processes these solutes must still provide appreciable osmotic pressure. Interestingly, structural features of various macromolecular species and molecular aggregates that allow for easy removal from aqueous solution can also serve to enhance osmotic pressure through nonideal solvent/solute interactions.

2.1. Osmotic pressure and FO water flux

The effects of osmotic pressure, solution viscosity, and molecular/ionic diffusivity on water flux (J_w) are shown in Eq. (1),

$$J_w = \frac{D\varepsilon}{t\tau} \ln \frac{B + A\pi_{D,m} - J_w}{B + A\pi_{F,b}} \quad (1)$$

where D is the diffusion coefficient of the solute (which decreases with solution viscosity); ε , t , and τ are the porosity, thickness, and tortuosity of the membrane support layer, respectively; B is the salt permeability coefficient of the membrane active layer; A is the pure water permeability coefficient; $\pi_{D,m}$ is the osmotic pressure of the draw solution at the membrane surface; and, $\pi_{F,b}$ is the osmotic pressure of the feed solution in the bulk [37]. Water flux increases with

increasing osmotic pressure difference ($\pi_{D,m} - \pi_{F,b}$), however the relationship is nonlinear because of ICP. As Eq. (1) demonstrates, draw solution osmotic pressure is the principal driving force in FO processes.

2.2. Thermodynamic basis of osmotic pressure

Consider an FO process using a polymer solution as the osmotic agent. If a polymer solution is separated from pure water by a semipermeable membrane the movement of water through the barrier is explained in terms of the chemical potential of the water, μ_w , under isothermal conditions, as given in Eq. (2),

$$\mu_w(P, X) = \mu_w^o(P, X^o) + RT \ln(\alpha_w) \quad (2)$$

where P is pressure, X is solution composition, R is the gas constant, T is temperature, α_w is the activity of water in the solution, and the superscript "o" denotes standard conditions. For the derivation that follows α_w will be replaced with the mole fraction of water in solution, X_w . In **Figure 1**, water spontaneously moves from the left side to the right side because $\mu_{w, \text{left}} > \mu_{w, \text{right}}$. Alternatively, it is possible to prevent net water flow by increasing the external pressure on the polymer solution such that $\mu_{w, \text{left}} = \mu_{w, \text{right}}$. The amount by which the external pressure is increased to prevent net flow is termed the osmotic pressure, π , of the draw solution.

As Eq. (2) implies, it is reasonable to differentiate μ_w in terms of P and X_s (the mole fraction of solute) to obtain Eq. (3).

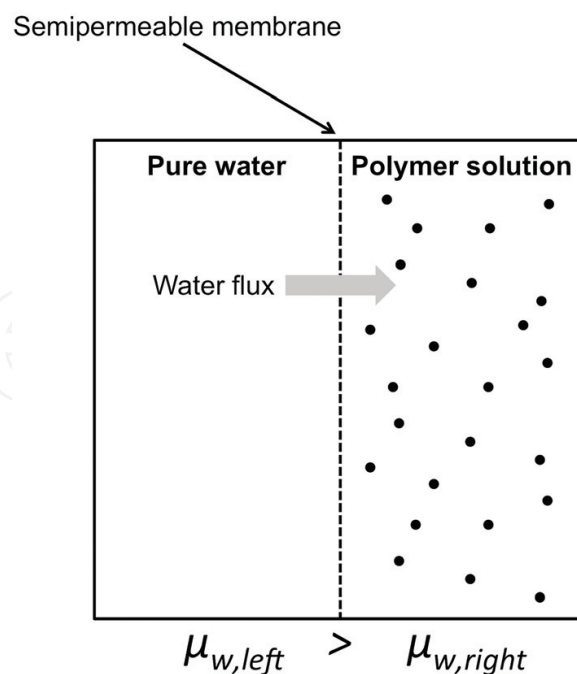


Figure 1. Osmotic behavior of an aqueous polymer solution.

$$d\mu_w = \left(\frac{\partial\mu_w}{\partial P}\right)_{T, X_s} dP + \left(\frac{\partial\mu_w}{\partial X_s}\right)_{T, P} dX_s \quad (3)$$

The definitions of Gibbs free energy and chemical potential are given by Eqs. (4) and (5), respectively,

$$G = H - TS \quad (4)$$

$$\mu_w = \left(\frac{\partial G}{\partial n_w}\right)_{T, P, n_s} \quad (5)$$

where H is enthalpy, S is entropy, n_w is moles of water, and n_s is moles of solute. Application of fundamental thermodynamics to a two-component solution of water and polymer solute, s , provides Eq. (6), in which V is the volume of solution.

$$dG = -SdT + VdP + \left(\frac{\partial G}{\partial n_w}\right)_{T, P, n_s} dn_w + \left(\frac{\partial G}{\partial n_s}\right)_{T, P, n_w} dn_s \quad (6)$$

Eq. (6) reveals that under conditions of constant temperature and solution composition, the derivative of Gibbs free energy with respect to pressure is given by Eq. (7).

$$\left(\frac{\partial G}{\partial P}\right)_{T, X} = V \quad (7)$$

By differentiating Eq. (5) with respect to pressure, while holding other variables constant, Eq. (8) is obtained.

$$\left(\frac{\partial\mu_w}{\partial P}\right)_{T, X} = \frac{\partial^2 G}{\partial P \partial n_w} \quad (8)$$

Similarly, by differentiating Eq. (7) with respect to amount of water Eq. (9) is obtained, in which V_{m_w} is the partial molar volume of water.

$$\frac{\partial^2 G}{\partial n_w \partial P} = \left(\frac{\partial V}{\partial n_w}\right) = V_{m_w} \quad (9)$$

Because of the symmetry of second derivatives, meaning the order of differentiation is inconsequential, the partial molar volume of water is also given by Eq. (10).

$$V_{m_w} = \left(\frac{\partial\mu_w}{\partial P}\right)_{T, X} \quad (10)$$

Next, differentiation of an analogous form of Eq. (2) with respect to X_w provides Eq. (11).

$$\left(\frac{\partial\mu_w}{\partial X_w}\right)_{T,P} = \frac{RT}{X_w} \quad (11)$$

Because $X_w = 1 - X_s$ and therefore $\frac{dX_w}{dX_s} = -1$, Eq. (12) can be obtained.

$$\left(\frac{\partial\mu_w}{\partial X_s}\right)_{T,P} = \left(\frac{\partial\mu_w}{\partial X_w}\right)_{T,P} \frac{dX_w}{dX_s} = -\frac{RT}{1 - X_s} \quad (12)$$

If there is no net flow of water in an apparatus like that depicted in **Figure 1**, $d\mu_w = 0$ providing Eq. (13).

$$\left(\frac{\partial\mu_w}{\partial P}\right)_{T,X_s} dP = -\left(\frac{\partial\mu_w}{\partial X_s}\right)_{T,P} dX_s \quad (13)$$

Substituting Eqs. (10) and (12) into Eq. (13) and then integrating provides Eq. (14).

$$\int_{P_0}^{P_0+\pi} V_{m_w} dP = RT \int_0^{X_s} \frac{dX_s}{1 - X_s} \quad (14)$$

Assuming the solution is incompressible (meaning that partial molar volume is independent of pressure) allows for simple integration providing Eq. (15).

$$\pi = -\frac{RT}{V_{m_w}} \ln(1 - X_s) = -\frac{RT}{V_{m_w}} \ln(X_w) \quad (15)$$

For dilute solutions ($X_s \ll 1$ and $n_s \ll n_w$) the approximations in Eqs. (16) and (17) are justified,

$$\ln(1 - X_s) \approx -X_s \quad (16)$$

$$X_s = \frac{n_s}{n_s + n_w} \approx \frac{n_s}{n_w} \quad (17)$$

which upon substitution into Eq. (15) provides the familiar van't Hoff equation, Eq. (18).

$$\pi V = n_s RT \quad (18)$$

Deviations of solution osmotic pressure data from Eq. (18) are generally attributable to nonideal solvent-solute and solute-solute interactions. One way of expressing the extent to which a solution deviates from ideality is through the osmotic coefficient, ϕ , which is defined on an amount fraction basis in Eq. (19).

$$\phi = \frac{\mu_w^0 - \mu_w}{RT \ln X_w} \quad (19)$$

The osmotic coefficient is analogous to the activity coefficient and can be defined in terms of other concentration units. It is often used in conjunction with i , which accounts for dissociation/ion-pairing, to provide Eq. (20), where C_s is the molar concentration of associated solute.

$$\pi = i\varphi C_s RT \quad (20)$$

Alternatively, and in particular for polymer solutions, solution osmotic pressure is often expressed as a power series expansion in C_s as in Eq. (21),

$$\pi = RT \left(\frac{C_s}{M_r} + A_2 C_s^2 + A_3 C_s^3 + \dots \right) \quad (21)$$

where M_r is molar mass and A_2 and A_3 are the second and third virial coefficients, respectively. These coefficients are temperature dependent, empirically determined constants for a given solvent system. In terms of the activity of water, α_w , osmotic pressure is perhaps best expressed as shown in Eq. (22).

$$\pi = -\frac{RT}{V_{m_w}} \ln(\alpha_w) \quad (22)$$

An empirical, semi-empirical, or theoretical methodology can then be used to relate α_w in Eq. (22) to X_w in Eq. (15). Given the significance of Eqs. (15) and (22), it is important to discuss the factors that effectively reduce the mole fraction of *free* water through hydration of solute species. The hydration number of a solute, h , influences X_w as shown in Eq. (23).

$$X_w = \frac{n_w - hn_s}{n_w - hn_s + in_s} \quad (23)$$

In terms of solute molality (C_{sm}), a concentration unit often reported in FO studies, the hydration number of a solute, h , can be incorporated as shown in Eq. (24),

$$C_{sm} = \frac{n_s}{M_w - (hn_s \times 0.018015)} \quad (24)$$

where M_w is the total mass of water in the solution in kg. Solutes with greater h values produce solutions with higher osmotic pressures at a given concentration and are potentially better draw agents in FO processes, though viscosity considerations are also very important.

2.3. Osmotic pressure of aqueous solutions of inorganic salts

Wilson and Stewart [38] have provided a good discussion of how solution osmotic pressure is affected by the hydration of simple ionic compounds. The short range interactions between electron pairs in water molecules and cations lead to h values that can range from, for example, 1.8 for NH_4^+ to 13 for Mg^{2+} [39]. To illustrate the influence of hydration, consider the comparison of aqueous solutions of NaCl and KCl as osmotic agents. Achilli et al. [11] determined the concentrations of NaCl and KCl required to achieve a solution osmotic pressure of 44 atm and also the corresponding J_w values for these solutions. **Table 1** provides the results of using Eqs. (15) and (23), with literature values [40] for h and i , to calculate osmotic pressures. The sodium ion's smaller size and corresponding higher charge density impart a larger h value,

Compound	Molarity	h	i	X_w	π (atm)	J_w (m/s)
NaCl	0.869	3.9	1.84	0.968	44	3.38×10^{-6}
KCl	0.943	1.7	1.85	0.968	44	3.74×10^{-6}

Table 1. Osmotic properties of aqueous solutions of NaCl and KCl [11, 40].

allowing NaCl solutions to achieve a given osmotic pressure at a lower concentration than KCl solutions.

In terms of osmotic pressure and corresponding FO performance there are diminishing returns on using ever-higher concentrations of ionic compounds, especially when increased solution viscosity is also considered. While hydration numbers tend to increase with increasing cation charge density, they decrease with increasing concentration, owing in part to increased ion-pairing, effectively reducing i . The hydration of molecular aggregates or macromolecular species and its corresponding effect on solution osmotic pressure has also been extensively studied, especially for systems consisting of poly(ethylene glycol) (PEG), DNA, chondroitin sulfate, and BSA [31–35, 41, 42]. These studies provide valuable insights into FO processes using molecular aggregates or macromolecular species as draw agents, especially those incorporating MNPs.

2.4. Osmotic properties of aqueous solutions of large organic molecules

In their studies of BSA, Kanal et al. [32] observed that osmotic pressure decreases as solution pH increases from 3 to approximately 4.6 and then increases with pH. Increases in osmotic pressure on either side of the minimum are attributed to increased electrostatic repulsive interactions. At pH values below the isoelectric point ($pI_{BSA} = 5.4$), the protein adopts a net positive charge along its surface. At pH values above pI_{BSA} , it is net negative. Electrostatic repulsion leads to a less compact protein conformation, greater segmental motion, more effective hydration, and higher osmotic pressures. Near the isoelectric point, the net-neutral protein strands adopt a more compact configuration, are less hydrated, and even tend to aggregate due to reduced intermolecular repulsion. The osmotic nonideality of BSA solutions is generally attributable to two sources: (1) large solvent/solute interactions that effectively increase polymer hydration (h) and (2) segmental motion of small portions of the polymer chains that effectively increase the number of particles in solution (i). Similar sources of nonideal behavior were also used to describe the osmotic properties of aqueous solutions of PEG [31, 43, 44].

The hydration of PEG of molecular weight 2000 Da (PEG^{2000}), both unattached and attached to distearoyl phosphoethanolamine liposomes ((DSEP)- PEG^{2000}), was investigated by Tirosh et al. [43]. Using differential scanning calorimetry, PEG^{2000} was found to bind 136 ± 4 water molecules, while (DSEP)- PEG^{2000} binds 210 ± 6 water molecules. In terms of hydration number per monomeric unit (approximately 46 units in 2000 Da PEG), these binding values correspond to hydration numbers of 3.0 and 4.6 for PEG^{2000} and (DSEP)- PEG^{2000} , respectively. The increase in water molecule binding is attributed to conformational changes, a coil configuration in PEG^{2000} and a brush configuration in (DSEP)- PEG^{2000} . When grafted to the liposome surface, the close

proximity of the polymeric strands causes them to repel each other and to adopt a more extended, easily hydrated, form. Such behavior has been exploited in the development of draw agents that incorporate superparamagnetic magnetite (Fe₃O₄) onto which polymers were grafted [19–28].

3. MNPs as FO draw agents

A summary of some recent applications of derivatized MNPs as draw agents in FO processes is provided in **Table 2**, which includes approximate concentrations of the repeating (monomeric) units used as capping agents on the MNPs. Other researchers have demonstrated that the osmotic properties of aqueous polymer solutions are perhaps best interpreted in terms of monomer concentration [31, 45].

Coating agent	Size (nm)	[Monomer] (M)	J_w (LMH)	π (atm)	Ref.
2-Pyrrolidine	28	0.15	4.6	17	[20]
TREG	24	0.20	5.8	23	
PAA ¹⁸⁰⁰	21	1.0	7.6	36	
Dextran	10	11	8.9	N/A	[21]
PEG ²⁵⁰ -(COOH) ₂	11.7	0.37	N/A	73	[22]
PEG ⁶⁰⁰ -(COOH) ₂	13.5	0.88	9.1	66	
PEG ⁴⁰⁰⁰ -(COOH) ₂	17.5	5.9	N/A	55	
PAA ¹⁸⁰⁰	5	1.5	11.2	70	[46]
PAA ¹⁸⁰⁰	20	N/A	N/A	18	[23]
PNaAA ¹⁸⁰⁰	20	N/A	2.1	32	
PCaAA ¹⁸⁰⁰	20	N/A	1.8	27	
PNaSS-PNIPAM	5	2.3	14.9	55.0	[26]
	9	2.5	9.9	40.8	
Citrate	3–8	0.015	16	N/A	[27]
HPG	20.9	2.1	6.7	15	[28]
PNaAA ²¹⁰⁰	9	0.0083	5.3	11.4	[24]
Citric acid	40	0.52	12.7	64	[19]
Oxalic acid	35	0.84	10.3	47	
PNaAA	160	12.4	N/A	19.5	[25]
Si-COOH	12.7	0.046	1.7	6.3	[47]
Si-PEG ⁵³⁰	13.6	0.43	2.0	7.6	

Abbreviations: TREG: triethylene glycol; PAA: poly(acrylic acid); PEG-(COOH)₂: poly(ethylene glycol) diacid; PNaAA: poly(sodium acrylate); PCaAA: poly(calcium acrylate); PNaSS-PNIPAM: poly(sodium styrene-4-sulfonate) and poly(N-isopropylacrylamide) [15% PNaSS, 85% PNIPAM]; HPG: hyperbranched polyglycerol; Si-COOH: N-(trinethoxysilylpropyl)ethylenediamine triacetic acid; Si-PEG: 2-[methoxy-(polyethyleneoxy)propyl]trimethoxysilane. Superscripts represent the average molecular weights of polymeric stands.

Table 2. Summary of MNP-based draw agents used in FO processes.

3.1. Osmotic behavior of draw agents alone vs. grafted onto MNPs

Some investigators have studied the FO properties of osmotic agents that are both alone in aqueous solution and grafted onto MNPs [20, 24]. Ling et al. [20] compared 2-pyrrolidine, TREG, and PAA as draw solutes. When grafted onto MNPs, 2-pyrrolidine exhibited a near sixfold increase in osmolality when compared to the ungrafted solute. TREG and PAA exhibited approximately threefold and thirtyfold increases in osmolalities, respectively, at similar concentrations when grafted onto MNPs. Dey and Izake [24] found that 3.5 wt.% PNaAA provided a FO-water flux value of 1.72 LMH while only 0.078 wt.% PNaAA grafted onto MNPs provided a flux value of 5.32 LMH. These results indicate that anchoring polymers onto nanoparticles serves to significantly improve their osmotic performance.

The tremendous enhancement to osmotic pressure and water flux values associated with polymeric solutes anchored to MNPs can be attributed to improved hydration of the polymeric strands. The dense packing of polymer chains around MNPs leads to a more extended, brush-like, conformation due to excluded volume interactions [48, 49]. In addition, Ling et al. [20] ascribe a reduced interaction between PAA-MNPs and the FO-membrane surface as also contributing to the improved performance; carboxyl groups interacting with ester moieties on the membrane surface are not interacting with water and thereby reducing its chemical potential.

3.2. A semiempirical model

While h values can serve as a good assessment of changes in solution ideality, simply using Eqs. (15) and (23) to calculate h requires highly precise measurements of amount and osmotic pressure. Such measurements are likely not practical for osmotic systems incorporating macromolecular species or derivatized MNPs in FO. Fortunately, Fullerton et al. [50] proposed using Eq. (25) to model the osmotic behavior of proteins,

$$\frac{M_w}{M_s} = S \times \frac{1}{\pi} + I \quad (25)$$

where M_w is the mass of water, M_s is the mass of solute, and the two fitting parameters, S and I , are assessments of nonideality. The slope is given by Eq. (26),

$$S = \frac{RT\rho}{A_e} \quad (26)$$

where ρ is the density of water at temperature, T , and A_e is the effective osmotic molecular weight. Parameter I is a measure of solvent/solute interactions and is interpreted as varying directly with solvent-accessible surface area. The model and fitting parameters have been shown to adequately explain the solution properties of macromolecular solutes like BSA [32, 35] and PEG [31]. A free-solvent model proposed by Yousef et al. [51] that uses mole fraction as a measure of composition may also prove useful in analyzing nonidealities and has been shown effective particularly at high solute concentrations.

Figure 2 depicts the application of Eq. (25) to data for TREG [20, 31, 52] both alone in solution and grafted to MNPs. The ungrafted TREG molecules display little deviation from ideality,

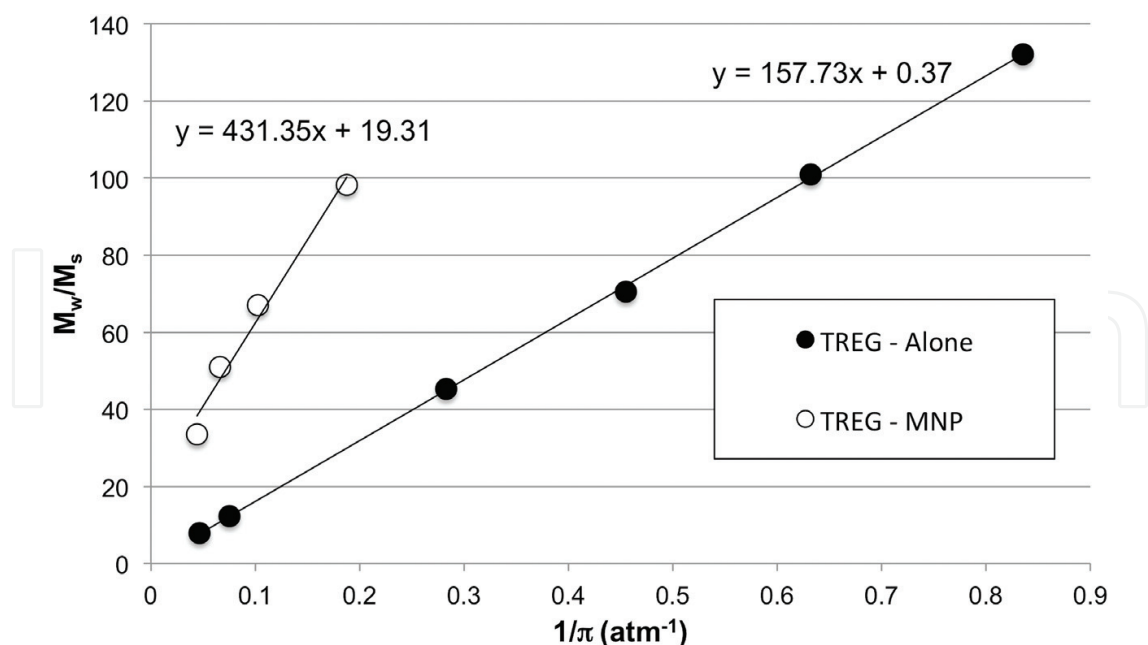


Figure 2. Nonideality analyses for TREG, using data from [20, 31, 52].

with a relatively small I value (0.37) and an effective osmotic molecular weight (153 g mol^{-1}) that is very close to the true molecular weight (150 g mol^{-1}). Though available data is somewhat limited, when grafted, nonideality appears to increase significantly. The value for I (19.3) is quite large when compared to values typically obtained for BSA ($\sim 4\text{--}12$) [35] and for PEG ($\sim 1\text{--}4$) [31], likely resulting from an increase in the amount of water in hydration shells around MNPs when compared to ungrafted TREG. The value for A_e (56.1 g mol^{-1}) is significantly lower than the value for the anchored trimer (149 g mol^{-1}), indicating that the grafted molecule behaves in solution as much smaller molecules.

The application of Eq. (25) to data for which 2-[methoxy-(polyethyleneoxy)_{6–9}propyl] trimethoxysilane (MW: $459\text{--}591 \text{ g mol}^{-1}$) was used as the grafting agent [47] is provided in **Figure 3**. When compared to TREG data, the greater number of monomers per polymeric strand results in a smaller I value (5.8) and a larger A_e value (101 g mol^{-1}). Although there are differences in particle size and attachment group, these data seem to demonstrate that polymer molar mass affects osmotic performance. Ge et al. [22] found that MNPs coated with PEG²⁵⁰-(COOH)₂ provided the best FO performance when compared to similar grafting agents of larger molar mass, observing lower osmotic pressures per monomer concentration as polymer length increased. This difference is perhaps attributable to limited interactions between shorter grafted polymeric strands when compared to longer. Because of the close proximity of individual strands when attached to MNPs, longer strands may be more likely to become intertwined with neighboring strands, thus reducing the surface area available for hydration. Interestingly, the opposite trend has been observed for ungrafted PEGs in the range 200 Da to 10,000 Da, with I values generally increasing with molecular weight before leveling off [31]. Ge et al. [22] also found that MNP-dispersibility increases with polymer length. Optimizing FO performance requires balancing the competing effects of polymer size on dispersibility, osmotic pressure, and viscosity.

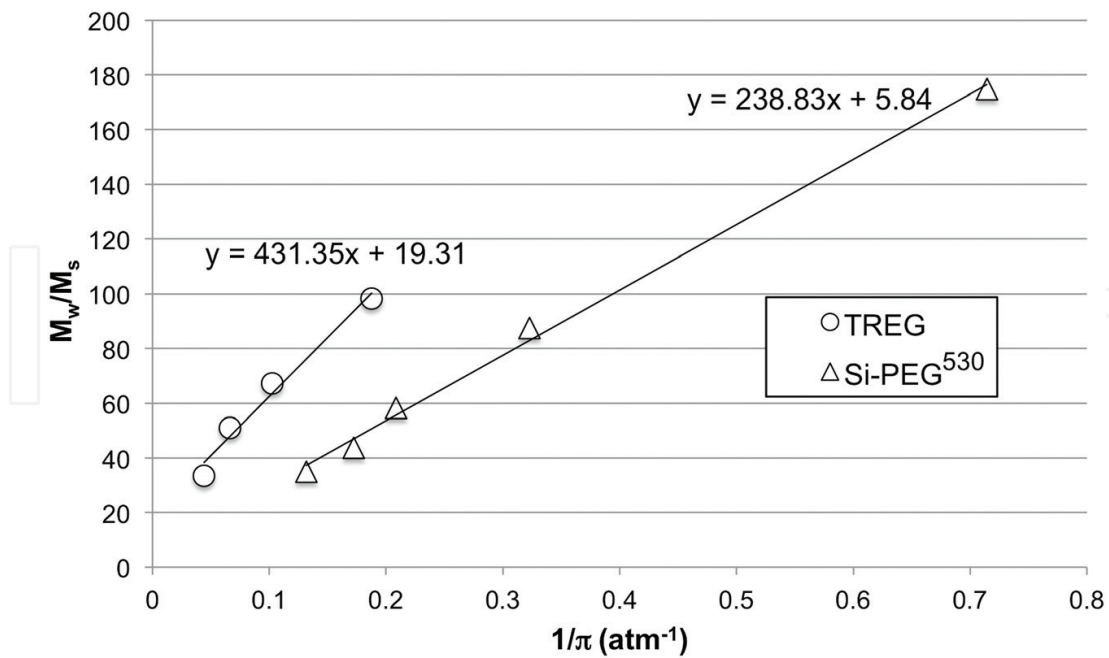


Figure 3. Nonideality analyses for TREG and Si-PEG⁵³⁰, using data from [20, 31, 47, 52].

In Figure 4, data for MNPs coated with PAA [20] and HPG [28] are depicted. These results again demonstrate the significant nonideal solution behavior of derivatized MNPs. The large A_e and small I values associated with HPG seem to indicate that the sprawling network of ether linkages may hinder hydration on a per gram of grafting agent basis. By comparison, the long, filamentous PAA¹⁸⁰⁰ strands provide an A_e value of 111 g mol⁻¹, which is intermediate between the

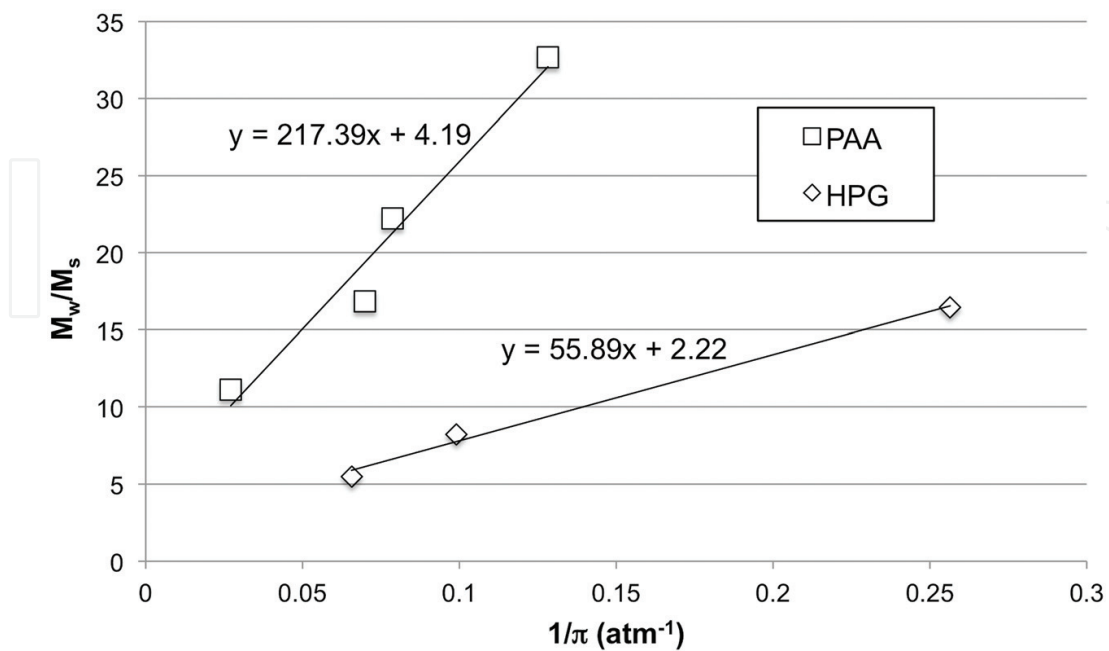


Figure 4. Nonideality analyses for HPG and PAA¹⁸⁰⁰, using data from [20, 28].

Osmotic agent	I	A_e	Ref.
TREG-alone	0.37	153	[20, 31, 52]
TREG-MNP	19.3	56.1	[20]
Si-PEG ⁵³⁰ -MNP	5.8	101	[47]
PAA ¹⁸⁰⁰ -MNP	4.2	111	[46]
HPG-MNP	2.2	433	[28]

Table 3. Summary of I and A_e values.

repeating monomer (72 g mol^{-1}) and the full polymer molecular weight (1800 g mol^{-1}). Several researchers [23–25] have also explored PNaAA as an MNP coating agent. Polyelectrolytes exploit greater i values to reduce X_w , however, the extent of ion-pairing between monomer units and counterions greatly influences solution osmotic pressure (**Table 3**).

3.3. Counterion binding

Another significant contributing factor to the osmotic potential of draw solutions incorporating polyelectrolytes is counterion binding. Oosawa was among the first to introduce the concept of counterion condensation around a polyion [53]. His model considers a fraction of counterions that is *bound* to the polyelectrolyte and the remainder is *unbound* in the bulk aqueous phase. Oosawa’s expression, provided in Eq.(27), relates the degree of polyelectrolyte dissociation, β ; the apparent volume fraction in which counterions are located, ϕ ; the absolute value of charge on the counterion, z ; and, the intensity of the potential at the polymer surface, Q .

$$\ln\left(\frac{1-\beta}{\beta}\right) = \ln\left(\frac{\phi}{1-\phi}\right) + \beta z Q \ln\left(\frac{1}{\phi}\right) \quad (27)$$

Using this model, bound counterions would not contribute to osmotic pressure while unbound ions would. Polymeric structural features that influence the magnitude of Q would therefore significantly impact the osmotic properties of solutions containing that polymer, either alone or grafted onto MNPs. Gwak et al. [54] demonstrated that poly(sodium aspartate) (PNaAsp) provided better osmotic performance than PNaAA, a result attributed to greater polyelectrolyte dissociation (larger β) in the case of PNaAsp. The larger spacing between charged moieties on PNaAsp strands results in a lower surface potential and therefore a higher degree of unbound counterions. Tian et al. [55] investigated the use of ungrafted PNaSS as a draw solute in FO, observing that conductivity and osmotic pressure increase with increasing PNaSS molecular weight, particularly at higher molecular weights. These results indicate that β and Q vary with polymer molecular weight.

3.4. Particle size

Data also indicate that MNP particle size influences their osmotic performance because smaller particles have a larger surface area per volume, thus allowing for more effective grafting-agent coverage and increased nonideality. Ling et al. [20] demonstrated the inverse relationship

between nanoparticle size and osmolality using PAA-MNPs. However, Kim et al. [56] found that particles smaller than 11 nm were difficult to separate from solution even with the application of a strong magnetic field, while the removal of particles larger than about 20 nm from the magnetic separator column was problematic. Additionally, the larger the mass percentage of coating material on a Fe_3O_4 core, the lower the saturated magnetization value on a per gram of particle basis. More coating material likely imparts greater osmotic pressure, but it reduces the efficacy of separation. Another significant challenge associated with MNP draw agents is particle aggregation following magnetic separation.

Ge et al. [22] observed a flux decline to approximately 80% of its original value after 9 recycles; this flux decline was accompanied by a particle size increase to 141% of the original value. That study used MNPs with an initial diameter <20 nm. Mino et al. [25] used much larger particles, with diameters of approximately 160 nm, and observed no aggregation even after 10 recycles, though the larger particles achieved only modest osmotic pressures. Park et al. [47] demonstrated that Si-PEG⁵³⁰-MNPs ($\text{diameter}_{\text{initial}} = 13.6$ nm) showed no significant aggregation or FO performance decline after 8 recycles, while Si-COOH-MNPs displayed considerable aggregation after only 5 recycles. Aggregation of the Si-COOH-MNPs was attributed to strong hydrogen bonding between carboxylate groups on adjacent particles when brought into close proximity during magnetic separation and subsequent drying. The oxalic acid- and citric acid-coated MNPs studied by Ge et al. [19] showed no significant particle agglomeration during regeneration, likely the result of strong electrostatic repulsion between particles. Zhao et al. [26] also observed only a slight decline in water flux ($<10\%$) following recycles of their negatively charged PNaSS-PNIPAM-coated particles. In addition, Na et al. [27] demonstrated that small MNPs (3–8 nm) penetrate pores within the FO-membrane support layer (10–40 nm) and become lodged leading to a decline in flux values with time.

4. Summary

While it is now generally accepted that FO processes do not offer an overall energy cost savings when compared to RO for seawater desalination, the prospects of niche applications for FO where RO is unsuitable are numerous. A major challenge for the wider use of FO technology is the development of draw agents that provide high water flux, low reverse solute flux, and facile recovery. Organic-coated superparamagnetic nanoparticles provide properties that address these requirements. The FO performance of MNPs is a function of coating material, particle size, and concentration; with mitigation of particle aggregation during recovery being an essential consideration. The osmotic performance of organic compounds improves significantly when grafted onto MNPs, likely resulting from increased solvent-accessible surface area and enhanced hydration. Application of a simple semiempirical model provides assessments of the nonideality associated with MNPs through calculation of a solvent/solute interaction parameter (I) and the effective osmotic molecular weight (A_e). When attached to MNPs, polymers behave osmotically as much smaller molecules. MNPs derivatized with filamentous, charged molecules (i.e. PNaAA) seem to provide the best results, both in terms of water flux and recoverability. Other significant contributing factors to the overall efficacy of

MNP-based draw solutions are particle size and the extent of counterion binding, with particles in the range 10–20 nm, coated with polyelectrolytes demonstrating high degrees of dissociation, proving most favorable. While the search for the *ideal* draw solute will certainly continue, organic-coated MNPs, because of their enhanced nonideal behavior, offer an encouraging avenue of possibility and opportunity.

Acknowledgements

Support for this work was provided by the Qatar Foundation and was made possible in part by a grant from the Qatar National Research Fund under its Undergraduate Research Experience Program award no. UREP13-018-1-001. Its contents are solely the responsibility of the authors and do not necessarily represent the official views of the Qatar National Research Fund.

Author details

Jimmy D. Roach*, Mandy M. Bondaruk and Zain Burney

*Address all correspondence to: jar2038@qatar-med.cornell.edu

Pre-Medical Education Unit, Weill Cornell Medicine-Qatar, Doha, Qatar

References

- [1] Zhao S, Zou L, Tang CY, Mulcahy D. Recent developments in forward osmosis: Opportunities and challenges. *Journal of Membrane Science*. 2012;**396**:1-21
- [2] Klaysom C, Cath TY, Depuydt T, Vankelecom IF. Forward and pressure retarded osmosis: Potential solutions for global challenges in energy and water supply. *Chemical Society Reviews*. 2013;**42**:6959-6989
- [3] Phuntsho S, Sahebi S, Majeed T, Lotfi F, Kim JE, Shon HK. Assessing the major factors affecting the performances of forward osmosis and its implications on the desalination process. *Chemical Engineering Journal*. 2013;**231**:484-496
- [4] Shaffer DL, Werber JR, Jaramillo H, Lin S, Elimelech M. Forward osmosis: Where are we now? *Desalination*. 2015;**356**:271-284
- [5] Akther N, Sodiq A, Giwa A, Daer S, Arafat HA, Hasan SW. Recent advancements in forward osmosis desalination: A review. *Chemical Engineering Journal*. 2015;**281**:502-522
- [6] Qasim M, Darwish NA, Sarp S, Hilal N. Water desalination by forward (direct) osmosis phenomenon: A comprehensive review. *Desalination*. 2015;**374**:47-69

- [7] Cai Y, Hu X. A critical review on draw solutes development for forward osmosis. *Desalination*. 2016;**391**:16-29
- [8] Cath TY, Elimelech M, McCutcheon JR, McGinnis RL, Achilli A, Anastasio D, Brady AR, Childress AE, Farr IV, Hancock NT, Lampi J, Nghiem LD, Xie M, Yip NY. Standard methodology for evaluating membrane performance in osmotically driven membrane processes. *Desalination*. 2013;**312**:31-38
- [9] Wei J, Qiu C, Tang CY, Wang R, Fane AG. Synthesis and characterization of flat-sheet thin film composite forward osmosis membranes. *Journal of Membrane Science*. 2011;**372**:292-302
- [10] Alejo T, Arruebo M, Carcelen V, Monsalvo VM, Sebastian V. Advances in draw solutes for forward osmosis: Hybrid organic-inorganic nanoparticles and conventional solutes. *Chemical Engineering Journal*. 2017;**309**:738-752
- [11] Achilli A, Cath TY, Childress AE. Selection of inorganic-based draw solutions for forward osmosis applications. *Journal of Membrane Science*. 2010;**364**:233-241
- [12] Ge Q, Su J, Amy GL, Chung T-L. Exploration of polyelectrolytes as draw solutes in forward osmosis processes. *Water Research*. 2012;**46**:1318-1326
- [13] Lecaros RLG, Syu Z-C, Chiao Y-H, Wickranasinghe SR, Ji Y-L, An Q-F, Hung W-S, Hu C-C, Lee K-R, Lai J-Y. Characterization of a thermoresponsive chitosan derivative as a potential draw solute for forward osmosis. *Environmental Science & Technology*. 2016;**50**:11935-11942
- [14] McCutcheon JR, McGinnis RL, Elimelech M. Desalination by ammonia-carbon dioxide forward osmosis: Influence of draw and feed solution concentrations on process performance. *Journal of Membrane Science*. 2006;**278**:114-123
- [15] Wang Y, Yu H, Xie R, Zhao K, Ju X, Wang W, Liu Z, Chu L. An easily recoverable thermo-sensitive polyelectrolyte as draw agent for forward osmosis process. *Chinese Journal of Chemical Engineering*. 2016;**24**:86-93
- [16] Roach JD, Al-Abdulmalek A, Al-Naama A, Haji M. Use of micellar solutions as draw agents in forward osmosis. *Journal of Surfactants and Detergents*. 2014;**17**:1241-1248
- [17] Li D, Zhang XY, Yao JF, Simon GP, Wang HT. Stimuli-responsive polymer hydrogels as a new class of draw agent for forward osmosis desalination. *Chemical Communications*. 2011;**47**:1710-1712
- [18] Li D, Wang H. Smart draw agents for emerging forward osmosis application. *Journal of Materials Chemistry A*. 2013;**1**:14049-14060
- [19] Ge Q, Yang L, Cai J, Xu W, Chen Q, Liu M. Hydroacid magnetic nanoparticles in forward osmosis for seawater desalination and efficient regeneration via integrated magnetic and membrane separations. *Journal of Membrane Science*. 2016;**520**:550-559
- [20] Ling MM, Wang KY, Chung T-S. Highly water-soluble magnetic nanoparticles as novel draw solutes in forward osmosis for water reuse. *Industrial & Engineering Chemistry Research*. 2010;**49**:5869-5876

- [21] Bai H, Liu Z, Sun DD. Highly water soluble and recovered dextran coated Fe₃O₄ magnetic nanoparticles for brackish water desalination. *Separation and Purification Technology*. 2011;**81**:392-399
- [22] Ge Q, Su J, Chung T-S, Amy G. Hydrophilic supermagnetic nanoparticles: Synthesis, characterization, and performance in forward osmosis. *Industrial & Engineering Chemistry Research*. 2011;**50**:382-388
- [23] Ling MM, Chung T-S. Surface-dissociated nanoparticle draw solutions in forward osmosis and the regeneration in an integrated electric field and nanofiltration system. *Industrial & Engineering Chemistry Research*. 2012;**51**:15463-15471
- [24] Dey P, Izake EL. Magnetic nanoparticles boosting the osmotic efficiency of a polymeric FO draw agent: Effect of polymer conformation. *Desalination*. 2015;**373**:79-85
- [25] Mino Y, Ogawa D, Matsuyama H. Functional magnetic particles providing osmotic pressure as reusable draw solutes in forward osmosis membrane process. *Advanced Powder Technology*. 2016;**27**:2136-2144
- [26] Zhao Q, Chen N, Zhao D, Lu X. Thermoresponsive magnetic nanoparticles for seawater desalination. *ACS Applied Materials & Interfaces*. 2013;**5**:11453-11461
- [27] Na Y, Yang S, Lee S. Evaluation of citrate-coated magnetic nanoparticles as draw solute for forward osmosis. *Desalination*. 2014;**347**:34-42
- [28] Yang H-M, Seo B-K, Lee K-W, Moon J-K. Hyperbranched polyglycerol-coated magnetic nanoparticles as draw solute in forward osmosis. *Asian Journal of Chemistry*. 2014;**26**:4031-4034
- [29] Beaman DK, Robertson EJ, Richmond GL. From head to tail: Structure, solvation, and hydrogen bonding of carboxylate surfactants at the organic–water interface. *Journal of Physical Chemistry C*. 2011;**115**:12508-12516
- [30] Wills PR, Scott DJ, Winzor DJ. Thermodynamics and thermodynamic nonideality. In: Roberts GK, editor. *Encyclopedia of Biophysics*. Springer; 2013. pp. 2583-2589
- [31] Zimmerman RJ, Chao H, Fullerton GD, Cameron IL. Solute/solvent interaction corrections account for non-ideal freezing point depression. *Journal of Biochemical and Biophysical Methods*. 1993;**26**:61-70
- [32] Kanal KM, Fullerton GD, Cameron IL. A study of the molecular sources of nonideal osmotic pressure of bovine serum albumin solutions as a function of pH. *Biophysical Journal*. 1994;**66**:153-160
- [33] Minton AP. A molecular model for the dependence of the osmotic pressure of bovine serum albumin upon concentration and pH. *Biophysical Chemistry*. 1995;**57**:65-70
- [34] Yousef MA, Datta R, Rodgers VGJ. Understanding nonidealities of the osmotic pressure of concentrated bovine serum albumin. *Journal of Colloid and Interface Science*. 1998;**207**:273-282

- [35] Zimmerman RJ, Kanal KM, Sanders J, Cameron IL, Fullerton GD. Osmotic pressure method to measure salt induced folding/unfolding of bovine serum albumin. *Journal of Biochemical and Biophysical Methods*. 1995;**30**:113-131
- [36] Yamada S, Tanaka M. Softness of some metal ions. *Journal of Inorganic and Nuclear Chemistry*. 1975;**37**:587-589
- [37] Loeb S, Titelman L, Korngold E, Freiman J. Effect of porous support fabric on osmosis through a Loeb-Sourirajan type asymmetric membrane. *Journal of Membrane Science*. 1997;**129**:243-249
- [38] Wilson AD, Stewart FF. Deriving osmotic pressures of draw solutes used in osmotically driven membrane processes. *Journal of Membrane Science*. 2013;**431**:205-211
- [39] Zavitsas AA. Properties of water solutions of electrolytes and nonelectrolytes. *Journal of Physical Chemistry B*. 2001;**105**:7805-7817
- [40] Marcus Y. *Ions in Solution and their Solvation*. Wiley; 2015. p. 140
- [41] Bathe M, Rutledge GC, Grodzinsky AJ, Tidor B. Osmotic pressure of aqueous chondroitin sulfate solution: A molecular modeling investigation. *Biophysical Journal*. 2005;**89**:2357-2371
- [42] Carrillo J-MY, Dobrynin AV. Salt effect on osmotic pressure of polyelectrolyte solutions: Simulation study. *Polymer*. 2014;**6**:1897-1913
- [43] Tirosh O, Barenholz Y, Katzhendler J, Prieve A. Hydration of polyethylene glycol-grafted liposomes. *Biophysical Journal*. 1998;**74**:1371-1379
- [44] Hansen PL, Cohen JA, Podgornik R, Parsegian VA. Osmotic properties of poly(ethylene glycols): Quantitative features of brush and bulk scaling laws. *Biophysical Journal*. 2003;**84**:350-355
- [45] Essafi W, Lafuma F, Baigl D, Williams CE. Anomalous counterion condensation in salt-free hydrophobic polyelectrolyte solutions: Osmotic pressure measurements. *Europhysics Letters*. 2005;**71**:938-944
- [46] Ling MM, Chung TS. Desalination process using super hydrophilic nanoparticles via forward osmosis integrated with ultrafiltration regeneration. *Desalination*. 2011;**278**:194-202
- [47] Park S-Y, Ahn H-W, Chung J-W, Kwak S-Y. Magnetic core-hydrophilic shell nanosphere as stability-enhanced draw solute for forward osmosis (FO) application. *Desalination*. 2016;**397**:22-29
- [48] Achilleos DS, Vamvakaki MV. End-grafted polymer chains onto inorganic nano-objects. *Materials*. 2010;**3**:1981-2026
- [49] Milner ST. Polymer brushes. *Science*. 1991;**251**:905-914

- [50] Fullerton GD, Zimmerman RJ, Cantu C, Cameron IL. New expressions to describe solution nonideality: Osmotic pressure, freezing-point depression and vapor pressure. *Journal of Biochemistry and Cell Biology*. 1992;**70**:1325-1331
- [51] Yousef MA, Datta R, Rodgers VGJ. Free-solvent model of osmotic pressure revisited: Application to concentrated IgG solution under physiological conditions. *Journal of Colloid and Interface Science*. 1998;**197**:108-118
- [52] Sun T, Teja A. Density, viscosity, and thermal conductivity of aqueous ethylene, diethylene, and triethylene glycol mixtures between 290 K and 450 K. *Journal of Chemical & Engineering Data*. 2003;**48**:198-202
- [53] Oosawa F. A simple theory of thermodynamic properties of polyelectrolyte solutions. *Journal of Polymer Science*. 1957;**23**:421-430
- [54] Gwak G, Jung B, Han S, Hong S. Evaluation of poly (aspartic acid sodium salt) as a draw solute for forward osmosis. *Water Research*. 2015;**80**:294-305
- [55] Tian E, Hu C, Qin Y, Ren Y, Wang X, Wang X, Xiao P, Yang X. A study of poly (sodium 4-styrenesulfonate) as draw solute in forward osmosis. *Desalination*. 2015;**360**:130-137
- [56] Kim YC, Han S, Hong S. A feasibility study of magnetic separation of magnetic nanoparticle for forward osmosis. *Water Science and Technology*. 2011;**64**:469-476

